Determination of the Fe−CO Bond Energy in Myoglobin Using Heterodyne-Detected Transient Thermal Phase Grating Spectroscopy

Markus Walther,[†,‡] Valerica Raicu,[§] Jennifer P. Ogilvie,[†,⊥] Ralph Phillips,[†] Ronald Kluger,[†] and R. J. Dwayne Miller*[,†]

Departments of Chemistry and Physics, and the Institute for Optical Sciences, University of Toronto, 80 St. George Street, Toronto, Ontario M5S 3H6, Canada, Department of Physics, University of Alberta, Edmonton, Alberta T6G 2J1, Canada, and Physics Department, University of Wisconsin−Milwaukee, Milwaukee, Wisconsin 53211

Received: May 5, 2005; In Final Form: August 19, 2005

The bond energies at active sites of proteins are intimately coupled to the structure−function relationship in biological systems. Due to the unknown nature of the protein relaxation along a reaction coordinate, it has not been possible to directly determine bond energies relevant to protein function. By embedding proteins in trehalose glasses, it is possible to freeze out protein relaxation on short time scales and determine the bond energies of photolabile ligands using photothermal spectroscopies. As a prototypical example, the photodissociation dynamics and energetics of carboxy-myoglobin (MbCO) in a trehalose glass matrix at room temperature were studied by transient absorption (or pump−probe) and transient thermal phase grating spectroscopy to determine the CO recombination dynamics and associated energetics, respectively. Both the initial energetics of the bond breaking and the energy released upon bond reformation could be used, on a time scale faster than significant protein relaxation, to determine the Fe−CO bond energy as 34 ± 4 kcal/mol. This bond energy is significantly larger than that typically cited (25 kcal/mol) on the basis of indirect measurements but is in good agreement with recent theoretical predictions (35 kcal/mol) (Rovira, C.; Parrinello, M. *Int. J. Quantum Chem.* **2000**, *80*, 1172). This result in combination with the theoretical study suggests that protein structure plays a significant role in the bond energies at active sites which in turn provides a tuning element of the effective barrier heights independent to the transition state region.

Introduction

Biological systems are driven by chemical reactions in which chemical energy stored as potential energy is released to execute a function as part of a complex series of coupled reaction processes. The specific three-dimensional structure of the protein is critical to protein activity in this regard. The protein structure is thought to be highly optimized through the evolutionary pressures of natural selection. However, the exact mechanism by which the protein structure mediates its influence on the course of reactions is open to debate. The structure can influence reaction pathways by affecting barrier heights, orientation, or entropic factors, as well as the overall driving force or free energy. Since biological systems are far from equilibrium, it is not possible to connect protein structure to the driving force alone. Kinetic factors are likely the key determinants in protein evolution. For this reason, the structure−function relationship of proteins is often discussed in terms of how the structure affects barrier heights or orientational (entropic) factors of forming an activated complex.[1] In other words, the primary focus is on how the protein structure affects the rate of passage through the reaction saddle point between the reactant and product surfaces. This line of reasoning has laid the foundation for synthetic approaches based on transition state analogues as a means to control protein/enzyme activity.[2] However, protein structure can also affect barrier heights by modifying the bond energy at an active site rather than stabilizing the transition state region. Structures that increase the bond energy at an active site effectively increase the barrier height to ligand dissociation and would thereby kinetically stabilize a ligand mediated reaction sequence (see Figure 1, inset). Conversely, structures that decrease the ligand bond energy at an active site would promote ligand release. All of these factors can be dynamic effects in which ligand binding and release are intimately related to structural changes around the active site. In fact, one should expect a global optimization of protein structure and dynamics with respect to kinetic factors that involve both the minima in the reactant/product surfaces and the barrier crossing region. To fully understand the structure−function relationship of proteins, we need detailed information about the bond energies at active sites in proteins. The latter information enables a global correlation of structure to the effective barrier heights and thereby helps separate entropic factors from enthalpic factors controlling the reaction pathway.

Measuring bond energies in biological systems remains an interesting experimental challenge that may resolve some important fundamental issues. How do structural differences affect bond energies at active sites? Is the primary effect of changes in protein structure to affect these bond energies? That is, could the variation in bond energies be the dominant forcing function for the evolution in protein structure? To resolve these questions, accurate determination of bond energies at ligation sites for different proteins are needed. This simple problem statement is complicated by medium effects. Accurate deter-

* Corresponding author. E-mail: dmiller@lphys.chem.utoronto.ca. Home page: http://lphys.chem.utoronto.ca.
[†] University of Toronto.
[‡] University of Alberta.
[§] University of Wisconsin−Milwaukee.
[⊥] Present address: Department of Physics, Biophysics Research Division, University of Michigan.

10.1021/jp052344n CCC: $30.25
Published on Web 10/11/2005

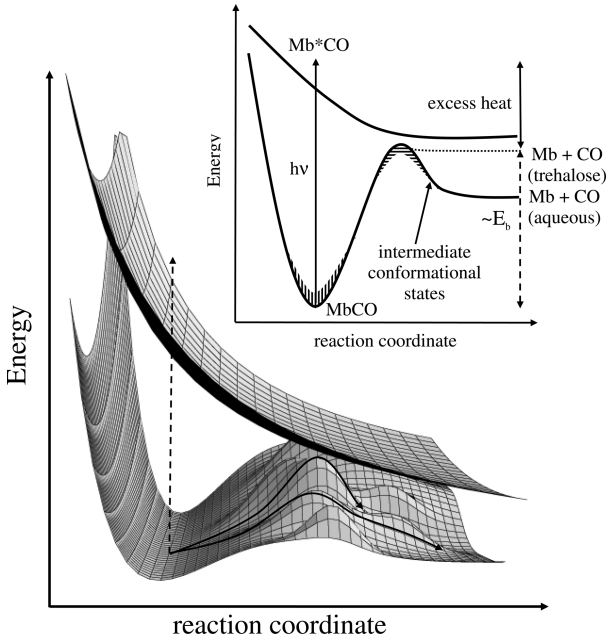

Figure 1. Photodissociation (dashed arrow) and thermal dissociation pathways (solid arrows) in MbCO. Inset: Upon excitation by a photon, the heme reaches an excited electronic state and the Fe−CO bond is broken. In trehalose, most subsequent protein relaxation is "frozen out", resulting in energy in excess of the bond energy, E_b, being released as heat. This allows a more accurate determination of E_b than a measurement made in aqueous solution, where Mb undergoes subsequent relaxation through intermediate states (not shown for simplicity) before the CO escapes the protein matrix. Through tuning of E_b (indicated by vertical hatched area), the protein structure can effectively raise or lower the barrier to ligand release. Similarly, control of ligand release can be achieved through stabilization of the transition state region (indicated by horizontal hatched area).

minations of bond energies are generally made in the gas phase to avoid complications from solvation effects.[3] For biological systems, the problem is more pronounced, as the heterogeneous nature of the chemistry makes it difficult to separate the energetics involved with changes in protein structure and aqueous repolarization/solvation energetics along a reaction coordinate. The conventional method of inferring bond energies is to use calorimetric measurements of a ligation reaction.[4−7] The problem is that the enthalpic measurements require an assumption about the degree of protein relaxation and differences in solvation enthalpy for the ligand in the protein and water. The differential solvation enthalpy can be estimated by comparing the enthalpy of solvation of the ligand in water and a nonpolar liquid as a model of the hydrophobic core of the protein.[6] The problem with this approach is the inherent assumption that the medium repolarization in nonpolar liquids (alkanes, benzene, etc.) is the same as that in proteins. While the protein core may be hydrophobic, proteins are fairly tightly packed structures. In fact, it remains a fundamental issue how even small ligands enter proteins at all given the degree of the structural perturbation required to create a void space large enough for the ligand. For example, on the basis of static structures, there is an estimated 30 kcal/mol barrier to the entry of ligands as small as CO or O_2 into heme proteins.[8] The solvation of a small ligand in nonpolar liquids in which only weak van der Waals forces are involved requires for the most part the development of a void space in the solution. There is very little perturbation in the alkane liquid structure outside the immediate solvation shell. In contrast, the introduction of a ligand into a protein requires considerable structural rearrangement of the strongly correlated atomic positions in proteins, in which even charged residues on the surface have to be displaced. Effectively, the forces involved in rearranging the protein structure to accommodate a ligand are much stronger than the weak forces involved in alkanes. These rearrangements have been dramatically revealed in recent time resolved X-ray studies where one can now observe the structure changes associated with ligand dissociation and escape from the protein with atomic resolution.[9] However, the energetics of this protein "solvation" or ligand entry and exit are not at all well understood. The energetics and the mass displacements are needed to fully understand the mechanics of functionally relevant protein motions. In this regard, there is likely considerable error in the assumptions used to estimate the enthalpy differences of the ligand in the protein and in solution in even estimating the relative contribution to protein relaxation along a reaction coordinate. The only quantitative information on the relevant protein energetics is available from transient photothermal measurements and only over limited ranges of the ligand escape.[10−16] A direct measurement of bond energies in biological systems is needed in which the protein relaxation energetics are decoupled from the energy balance equation.

This work takes advantage of the unique properties of heme proteins to provide a model system to explore the above issues connecting protein structure to function as it relates to the energetics driving biological processes. This class of proteins has well resolved structures as well as unique optical properties that make them conducive to photodissociation at the ligation site to initiate the reaction of interest.[17,18] In this regard, myoglobin (Mb) is the most well studied case. Small biologically important ligands such as O_2, NO, and CO bind to the heme Fe and can be selectively photoreleased with virtually unit quantum efficiency on sub-100 fs time scales.[19−21] This work focuses on the CO ligand, as there is less than 4% geminate recombination under physiological conditions.[22] These latter properties make carboxy-myoglobin (MbCO) very attractive for studies by photothermal methods[18,23] of the protein relaxation processes associated with ligand escape in which the full range of protein relaxation convolved to the ligand dissociation to escape from the protein can be dynamically mapped. In this regard, a quantitative determination of the Fe−CO bond energy will enable a determination of the relative importance of the different phases of the protein relaxation. In addition to these considerations, the Fe−CO bond energy of Mb provides an important test case for calorimetric methods and the advancement of first-principle theoretical methods for addressing protein energetics. The Fe−CO energy is considered to be a textbook case and is generally cited to be ∼25 kcal/mol on the basis of early calorimetric determinations as outlined above.[5−7] However, first-principle molecular dynamics simulations[24] predict a value as high as 35 kcal/mol. In these theoretical studies, no direct comparison to experimental work was given. However, it is clear from the relatively small sampling of different environments explored in the vicinity of the heme site in this study that the Fe-ligand bond energy is extremely sensitive to the local structure around the heme.

Motivated by the relatively large discrepancy between the theoretical studies and experimental estimates based on calorimetric data, the primary goal of the present study was to determine an accurate value for the ligand bond energy in MbCO. Again, the Fe−CO bond energy is also essential information for determining the relative contribution of the protein relaxation to the overall reaction coordinate. The bond energy was determined directly by the use of the recently developed heterodyne-detected transient grating spectros-

copy[15,25,26] in which the information on the energetics was isolated by exclusively probing the thermally induced changes in the index of refraction off resonance where thermal effects dominate the signal. This new approach is orders of magnitude more sensitive than previous transient thermal grating and related photothermal spectroscopies for the study of reaction energetics. The high sensitivity was essential to this study, as the protein motion convolved to the ligand dissociation coordinate must be frozen out of the problem to determine exclusively the Fe−CO bond energy. Removing the protein relaxation process from the energy balance was accomplished by embedding the protein in trehalose which has been shown to "freeze" protein relaxations over the time scale of interest while preserving the protein's structure and function.[27−30] The use of trehalose glass, however, makes it impossible to flow the sample, and the optical quality is greatly reduced from imperfections in the glass. This constraint places a premium on obtaining the highest signal-to-noise ratio possible to reduce the effect of laser noise from the associated large scattered light background. In this regard, heterodyne detection was an important advance toward making these experiments possible. Note that, by taking advantage of trehalose to remove the protein relaxation and the unit quantum yield for the photodissociation of CO, the Fe−CO bond energy is simply the difference in the photon energy and the amount of energy released from the protein to the trehalose matrix; all other nuclear relaxation processes are frozen out on the time scale of the observation of these experiments (see Figure 1). Furthermore, the Fe−CO bond energetics can be determined from subsequent geminate recombination under these conditions; that is, as long as the protein relaxation coordinate is fixed, the bond energy can be determined from both bond dissociation and bond formation pathways in this experiment. The reformation of the Fe−CO bond was quantified by independently determining the ground state recovery under identical conditions using transient absorption spectroscopy and correlating this rate of geminate recombination to the heat release observed in the heterodyne-detected transient phase grating studies. The use of this degenerate information helps increase the confidence in the determined bond energies.

The above experimental protocol provides a new general procedure for directly determining bond energies in biological systems without any inherent assumptions about the relative contribution of the protein relaxation/solvation to the overall energetics. This approach may be particularly timely, as it is only recently that computational techniques and computing power have advanced to the point where it is possible to directly solve the quantum mechanical equations for systems of sufficient complexity to provide useful information in a biological context. Myoglobin represents one of the few biological systems where numbers from first-principle simulations are currently available.[24] The present investigation and similar studies should provide valuable benchmarks for advancing theoretical models that will ultimately let us understand the energetics behind the structure−function relationship of biological systems at a microscopic level.

Materials and Methods

Sample Preparation. Horse muscle (heart) myoglobin and trehalose (α-D-glucopyranosil-α-D-glucopyranoside) were purchased from Sigma-Aldrich and used without further purification. Lyophilized ferric met-myoglobin (metMb) was dissolved (4 mM) in 0.2 M Tris buffer solution (pH 7) containing 0.27 M trehalose and then centrifuged at 12 000*g* for 10 min to remove impurities and undissolved parts. For the preparation of the MbCO sample, the solution was reduced with a 2-fold excess of sodium dithionite (Sigma) and equilibrated with CO at room temperature. A few drops of the solution were placed on a quartz window and subsequently dried for ∼4 h under a CO atmosphere in a silica gel desiccator. The sample was dried further and annealed in an oven at 353 K for 8 h, and was then sealed with another window and heated at 353 K for another 2−3 h. Aluminum foil was used as a spacer to control the sample thickness, which was adjusted so that an optical density of ∼1 was obtained for the sample at the probe wavelength (see below). Following this procedure, we obtained glassy samples of optical quality with no microcrystalline structure. The integrity of the embedded proteins was verified by UV−vis absorption spectroscopy.

Similar preparations of deoxyMb to serve as a control for a purely photothermal response were found to be too difficult to keep the iron in the reduced II deoxy state uniformly throughout the sample. Instead, malachite green was used as a control to characterize the photothermal response of trehalose. The samples of malachite green (MG) embedded in trehalose glass were prepared by mixing the dye with the same buffer solution and following the same drying and annealing steps as above.

Transient Absorption (Pump−Probe) Spectroscopy. Excitation light pulses (1 ns) were generated by a frequency-doubled (532 nm) Nd:YAG laser (VEM 1064-SW-50 microlaser) operating at a repetition rate of 3.5 kHz and a pulse energy of ∼1 μJ/pulse. The probe beam was provided by a He−Ne laser operating at a fundamental wavelength of 633 nm and at an output power of 0.63 mW. Both laser beams were focused onto the sample to spot sizes of 105 ± 10 μm for the excitation and 90 ± 10 μm for the probe beam. The transmitted probe intensity was measured with a fast photodiode (rise time ∼1 ns, Thorlabs) connected to a 500 MHz oscilloscope (Tektronix TDS 520D).

Thermal Phase Grating Spectroscopy. The heterodyne-detected four-wave mixing transient phase grating technique has been described in detail elsewhere.[15,26] Briefly, it uses two coherent (pulsed) beams intersecting at an angle in the sample to generate a transient interference grating. Changes in the complex refractive index are generated in the bright fringes, thus forming a physical grating in the sample material. Recording the diffraction efficiency[15] of an off-resonant probe beam incident on this transient grating permits observation of the time evolution of the complex refractive index, reflecting the structural and thermal dynamics of the sample. Our optical heterodyne detection (OHD) scheme, using diffractive optics, minimizes errors associated with phase instability of the mixed laser beams and their spatial jitter.[26] The same Nd:YAG laser as used for the transient absorption studies provided the excitation pulses (532 nm, 1 ns, 3.5 kHz repetition rate), while the off-resonant probe beam was generated by a diode pumped $Nd:YVO_4$ laser (Crystalaser) operating with 300 mW of cw output power at 1064 nm. The overlapped excitation and probe beams were focused to the desired spot sizes on a diffractive optic (DO) consisting of a phase grating (fringe spacing 7.5 μm). The ±1 diffractive order beams were collected with a spherical mirror and refocused onto the sample to spot sizes of 240 ± 10 μm for the excitation and 90 ± 10 μm for the IR probe beams. After crossing the sample, the part of the probe beam which is diffracted by the induced grating overlaps with the transmitted part of the second probe beam, and their detection by the same photodiode leads to large signal amplification through heterodyne mixing.[26] Two such signal/reference beam pairs were generated after the sample, and detection of

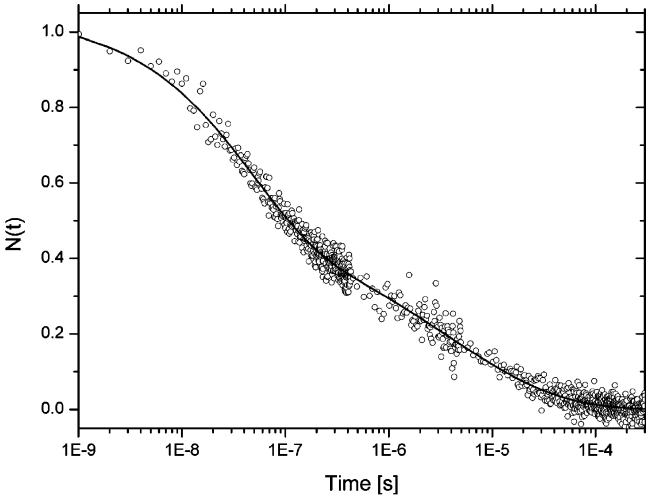

Figure 2. Ground state recovery. This plot gives the number of CO molecules not yet recombined after photodissociation, as determined by transient absorption spectroscopy. The solid line was simulated with eq 1 using the following best-fit parameter values: $N_1 = 0.51 \pm 0.03$, $k_1 = (2.29 \pm 0.13) \times 10^7\ s^{-1}$, $\beta_1 = 0.67 \pm 0.04$, $N_2 = 0.54 \pm 0.03$, $k_2 = (2.80 \pm 0.40) \times 10^5\ s^{-1}$, and $\beta_2 = 0.40 \pm 0.02$. The value of chi-square divided by the number of degrees of freedom (χ^2/d_f) was 0.22 for this fitting.

both by two separate fast photodiodes (Thorlabs PDA 155) followed by a differential measurement of the two resulting voltages helped increase the signal-to-noise ratio further. The real part of the signal, which was linearly proportional to the refractive index, was extracted by changing the relative phase between the diffracted and undiffracted beams through tilting a cover slip introduced on the path of one of the probe beams.[31]

Results and Discussion

Transient Absorption Spectroscopy. Weak transient absorption changes in the MbCO sample at wavelengths in the visible range are induced by photolysis of the bond between the CO ligand and heme Fe. In our case, absorption changes at 633 nm were used to monitor the temporal evolution of the ligated state of Mb. The transient absorption signal is directly related to the number of CO molecules dissociated from the heme iron, and its recovery directly reflects the rebinding of the ligand.

Figure 2 shows the dependence of the fraction of unbound CO molecules, $N(t)$, on the time, t, following photolysis. It was calculated from $N(t) = -\delta I(t)$, where δI is the normalized change in the transmitted intensity; $\delta I = -1$ corresponds to the maximal bleaching of the sample, which was ~4% in our experiments. As seen in Figure 2, two CO−Mb recombination steps are clearly distinguishable, although the distribution of reaction kinetic constants is highly stretched. In agreement with previously reported results, bimolecular rebinding (which is specific to Mb in fluid solvents and takes place on a longer time scale) was not observed in this study. This is indicated by the fact that $N(t)$ reaches a value of almost zero after less than 1 μs following photodissociation, suggesting that the glass matrix prohibits large amplitude motions of the protein, which would be necessary to enable ligand diffusion from one Mb molecule to another.

We simulated the recombination kinetics with a sum of two stretched exponentials (see solid line in Figure 2)

$$N(t) = N_1(0)e^{-(k_1 t)^{\beta_1}} + N_2(0)e^{-(k_2 t)^{\beta_2}} \qquad (1)$$

where k_1 and k_2 are two rate constants corresponding to the two recombination steps and β_1 and β_2 are empirical exponents. Equation 1 has been used with success previously in fitting Mb−CO recombination data from trehalose-embedded MbCO (see, e.g., Librizzi et al.[29] and references therein). Such nonexponential temporal evolution has been observed for myoglobin in various viscous media such as glycerol,[32] nanoporous silica gel,[33] or trehalose glass.[27−29]

The occurrence of two recombination processes may be thought to reflect either two energetic substates of the protein during a single recombination process or two parallel recombination processes of CO groups from two different sites within the heme pocket.[28,29,34] Regardless of the interpretation, we note the good overall agreement between our results and the published ones,[29] which provides valuable information for our determination of protein energetics (see below). It is worth mentioning here that we obtained fits of similar quality when using a sum of two power functions, which proved adequate previously for simulations of data from extremely dry samples.[29] However, for consistency with our analysis below of the transient grating data, we present here the parameter values obtained from fittings with the stretched exponential function (eq 1).

Transient absorption spectroscopy cannot be used directly to measure bond energies, as it only shows the kinetics of photodissociation and Mb−CO recombination (i.e., the phenomena occurring around the heme). However, the parameter values that this method provides (see the Figure 2 caption) will be used to reduce the number of fitting parameters in the analysis below of the transient grating data, which then allows determination of the bond energy.

Phase Grating Spectroscopy. As can be inferred from the Materials and Methods section, central to quantitative phase grating studies of photodissociable molecules is the ability to "write" a transient grating inside the solution containing the molecule of interest. This is achieved in our experiment by using optical excitation at 532 nm, which is absorbed by the sample and breaks the Fe−CO bond. A certain fraction of the absorbed photon energy goes toward breaking the Fe−CO bond, while the excess energy will be rapidly dissipated into the bath.[35] This causes density changes in the solvent through thermal expansion, which are detectable through measurements of the diffracted probe intensity. Our method for heterodyne-detected transient phase grating spectroscopy facilitates the measurement of very small amounts of energies involved in these processes with a resolution of better than 1 kcal.[15]

Figure 3 shows a typical phase grating signal (real part of the OHD signal) of MbCO in trehalose (open circles). In the inset, we show the corresponding signal of a MG sample. After some fast dynamics on nanosecond time scales related to contributions from excited state transitions and relaxation processes[36,37] in this high viscosity medium that interfere with the thermal grating signal, MG shows a pure thermal decay. Consequently, this system serves as a model of purely impulsive thermal grating response and is used in our paper to determine the thermal diffusion decay time for the experimental grating fringe spacing in the trehalose glass (see below).

Upon analyzing the MbCO data in Figure 3, we find that, within the first nanosecond, the light energy absorbed by the sample induces an abrupt index change due to thermal heating of the system, resulting in a non-zero grating signal different from 0. In the case of MG, essentially all the absorbed energy is released as heat; in MbCO, part of the energy is used to break the Fe−CO bond, and only the excess energy dissipates as heat into the solvent. Whereas MG shows on longer time scales a

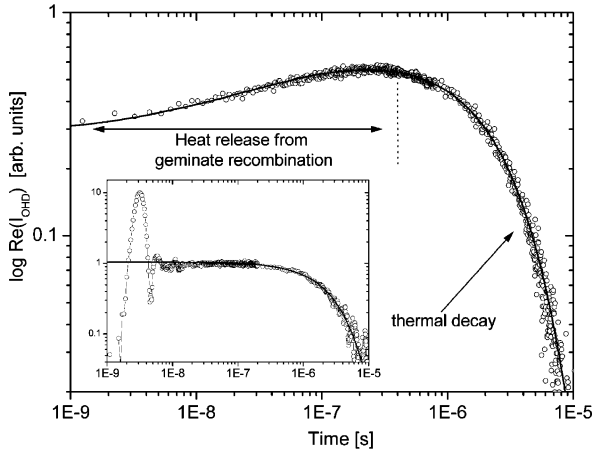

Figure 3. Measured diffraction grating signal of MbCO (open circles). Data errors are estimated to be ±0.03. The solid line was obtained from simulations with eq 2. The best-fit ($\chi^2/d_f = 0.23$) parameter values are the following: $A_{th} = 0.27 \pm 0.01$, $A_{th1} = 0.21 \pm 0.01$, $A_{th2} = 0.25 \pm 0.01$, while the other parameters—k_1, β_1, k_2, and β_2—were fixed to the values obtained from transient absorption measurements (see the Figure 2 caption). For the fit, we used the thermal grating decay time for this grating, $\tau_{th} = (2.40 \pm 0.02) \times 10^{-6}$ s, as determined from a single-exponential fit ($\chi^2/d_f = 0.59$) to the diffraction grating signal of malachite green (see solid line in the inset).

pure exponential decay due to thermal diffusion of the grating, the MbCO signal exhibits some additional dynamics. The diffracted signal increases by a factor of 2 on a time scale consistent with the fast geminate recombination rate identified in the transient absorption study (see above). For longer time, the MbCO signal decays due to thermal diffusion, similar to the behavior of the MG reference. On the basis of these observations, we model the time evolution of the grating signal by a sum of two stretched exponential decays corresponding to energy dissipation through two geminate recombination steps as found in the transient absorption studies (see eq 1), which is modulated by a thermal decay with a relaxation time τ_{th}:

$$\{Re\}(I_{OHD}) = \{A_{th} + A_{th1}[1 - e^{-(k_1 t)^{\beta_1}}] + A_{th2}[1 - e^{-(k_2 t)^{\beta_2}}]\}e^{-t/\tau_{th}} \quad (2)$$

In this equation, A_{th}, A_{th1}, and A_{th2} are the amplitudes of the thermal process and of the energy dissipation through the first and the second geminate recombination process. The other parameters are the same as those in eq 1. The thermal grating decay time, τ_{th}, has been determined from the MG reference by fitting a single-exponential decay to the data at longer times (solid line in the inset of Figure 3). Simulations of the phase grating signal with eq 2 produced the full line added to the MbCO data in Figure 3. For this purpose, we used τ_{th} from the MG fit (see the Figure 3 caption), and in order to limit the number of adjustable model parameters for MbCO, we kept the rates and the stretching constants fixed at the values obtained from the fitting to the pump−probe data (Figure 2).

From the resulting best-fit parameters, the Fe−CO bond energy in MbCO can now be estimated. Since the quantum yield of the CO dissociation in MbCO is nearly 1, we may assume that each absorbed photon breaks a bond. Thus, only the excess energy of the excitation pulse contributes to the initial heating of the solvent. This leads to a simple expression for the Fe−CO bond energy:

$$E_b = \left(1 - \frac{A_{th}}{A_{th} + A_{th1} + A_{th2}}\right)E_{h\nu} \quad (3)$$

where $E_{h\nu}$ is the excitation photon energy and the other parameters are as defined in eq 2.

Using the thermal amplitudes from the Figure 3 caption and an excitation energy of 54 kcal/mol for 532 nm photons, we calculate an Fe−CO bond energy of 34 ± 1 kcal/mol. Note that this error purely results from the errors of the fitting parameters. To test the fits for robustness against systematic errors introduced by using the parameters of the pump−probe fittings, we also performed an unconstrained fit where we let all parameters vary except for the thermal decay time to the phase grating signal. In this case, we obtained a value of 30 kcal/mol for the bond energy. The unconstrained fit, however, produces slightly longer geminate recombination times as observed in the pump−probe study (Figure 2). Because of this and due to the fact that a fit with too many unconstrained parameters leads to large errors, we regard this value as a lower limit for the Fe−CO bond energy. On the basis of these considerations, we report the Fe−CO bond energy to be 34 ± 4 kcal/mol as within the confidence limits of the measurement. This value is in good agreement with the results of the molecular dynamic simulations by Rovira and Parinello[24] (35 kcal/mol) and confirms that the protein is playing a very significant role in defining the bond energy at the active site.

Note that the reported rebinding energy of MbCO in trehalose has been determined on the basis of a model for the interpretation of our data, that we have used implicitly up to this point, which relies on the following assumptions: Although there are different time constants for the recombination, possibly associated with different recombination pathways, the enthalpy difference, E_b, between the dissociated and bound states is similar for all molecules. Furthermore, heat is only released upon rebinding; that is, there is no change in enthalpy due to transitions between two unbound states (e.g., passage from one (Xe−) cavity to another). The fact that the ratios of A_{th1}/A_{th2} in the fit to the thermal grating data and N_1/N_2 for the fit to the transient absorption data are very similar implies that all of the rebinding processes relevant for the transient grating response are equally captured by the pump−probe experiment, indicating that the above assumptions are indeed correct.

It is instructive to compare the large value for the Fe−CO binding energy obtained in the present study to the value of 25 kcal/mol for MbCO in aqueous solution determined in previous studies.[5,6] The difference between these two values (∼9 kcal/mol) accounts for the energy lost through additional protein relaxation of MbCO in aqueous solution. It is worth mentioning that, if residual protein relaxations are still present in the trehalose-coated Mb during the measurement, the bond energy that we reported above will be in fact an underestimate of the real value. This argues once more in favor of the value predicted by Rovira and Parinello.[24] The noted reorganization energy of the protein under physiological conditions undoubtedly involves displacements in the porphyrin ring, doming of the iron, and energy redistribution throughout the protein structure. These motions have recently been shown to be strongly coupled to the protein fluctuations[19,38−40] and are expected to be strongly attenuated in the highly viscous rigid trehalose environment. Such motions form the core of the functionally relevant motions under physiological conditions. In thinking about the energetics of these relaxation processes, the heme porphyrin can be considered to be the intramolecular coordinate for the ligand binding reaction and the surrounding protein matrix to be akin to the solvent in homogeneous reactions. The motions of the heavy atoms in the porphyrin ring (ν_4, ν_7 modes) and the out-of-plane Fe motion most strongly coupled to the bond breaking

are on the order of 0.1−0.3 Å, respectively.[19,41] Smaller but comparable motions occur through the protein matrix. It would be instructive to make a detailed accounting of the energetics with current basis sets for the interatomic potentials; however, such an estimate requires high resolution transient structures with the CO in the protein matrix. Protein relaxation processes associated with CO escape from the protein and penetration of water into the deoxy tertiary structure may largely off-set the overall enthalpy changes. High resolution transient structures capable of making this connection should soon be forthcoming from time resolved X-ray studies.[9] An estimate of the energetics based on the transient protein structures is outside the scope of the present work; however, we note that intramolecular reorganization energies involving similar displacements have been determined for a wide class of charge transfer reactions to be approximately 10 kcal (see, e.g., refs 42−44).

Protein relaxation energetics of this magnitude is at variance with the classical view that at most a few kilocalories per mole are stored in the protein structure in treating the energetics of this and related problems. It is further intriguing to consider the consequences of such significant protein relaxation in terms of kinetics. This relaxation would create an approximately 10 kcal/mol barrier to geminate recombination under physiological conditions in which these motions are part of the function. It has been argued that it is the protein relaxation that in fact helps expel CO from the heme site and is responsible for the very low geminate recombination of CO in aqueous media relative to O_2 and NO.[32,45,46] Previous temperature dependent studies of CO rebinding for such conditions have found the barrier to be 4−5 kcal/mol.[32] This determination appears to be in contradiction to the present findings in relation to the known enthalpic terms for MbCO. However, it needs to be noted that ligand photodissociation does not necessarily correspond to the same reaction coordinate/pathway as the fully thermally relaxed process and as such is not connected to the thermally relaxed ligand binding pathways, as indicated in Figure 1. For example, it is now accepted that CO quickly migrates to other regions within the protein, strongly correlated to Xe binding sites, from where it can recombine to the heme site.[9,10,47] It is interesting to speculate that ligand binding, in the wake of significant protein reorganization energies as inferred in this study, is governed by a convolution of the barrier distribution between different protein conformations and the associated barrier heights connecting conformations to ligation. The barriers separating the different conformations are independent of the barrier to ligand binding to first approximation; it is quite conceivable that fluctuations in a few labile degrees in the protein strongly modulate the barrier to ligand binding. The barriers to ligand access to the heme pocket on the distal side of the heme, illustrating exactly this effect, have been recently resolved using a combination of site directed mutants and media effects.[48] The proximal side of the heme principally governs the barrier height to ligation from within the heme pocket and coupling to the surrounding protein. In this case, thermal fluctuations leading to the displacement of the EF helix strongly modulate the out-of-plane motion of the iron and formation of the in-plane hexavalent iron in the ligand bound (oxy) state. This notion is the basis of allosteric regulation of haemoglobin and argues that such fluctuations are built into the protein architecture to govern function.[18] The present work makes this same connection in more general terms.

Conclusions

We investigated the photolysis and rebinding kinetics of carboxy-myoglobin (MbCO) embedded in a trehalose glass at room temperature using transient absorption and diffractive optics-based phase grating spectroscopy on nanosecond to microsecond time scales. From the pump−probe investigation, two rebinding processes were identified, which are interpreted in terms of geminate recombination of CO. Optical heterodyne-detected transient phase grating spectroscopy has been applied to measure the energetics of the photodissociation process. By fitting the transient grating data with an appropriate function, the branching of the excitation energy into ligand bond breaking and thermal heating was determined. Since additional energy losses through slow conformational relaxation of the protein are minimized by caging the molecule into a rigid trehalose glass matrix, the Fe−CO bond energy could be directly determined from our observations.

The bond energy obtained is larger than values determined in previous studies, which did not account for relaxation processes. Our result clearly favors the predictions by first-principle molecular dynamics simulations,[24] and it is, to our best knowledge, the most accurate experimental value for the Fe−CO binding energy in MbCO determined to date. Follow up studies with mutants will help to better elucidate the role of protein structure in mediating kinetics through stabilizing ground states and effective barrier heights. In a global optimization process, it is likely that the protein structure acts to stabilize ground states as well as transition state regions in the effective control of reaction kinetics. Studies of structure dependent bond energies will help to discern this structure−function connection.

Acknowledgment. This work was supported by the Natural Science and Engineering Research Council of Canada through an NSERC STRATEGIC grant. M.W. acknowledges funding by the Deutsche Forschungsgemeinschaft (DFG) through SFB 276, TP C14.

References and Notes

(1) Jencks, W. P. *Catalysis in chemistry and biology*; Dover Publications Inc.: New York, 1987.
(2) Schramm, V. L. *Acc. Chem. Res.* **2003**, *36*, 588.
(3) Blanksby, S. J.; Ellison, G. B. *Acc. Chem. Res.* **2003**, *36*, 255.
(4) Levine, I. N. *Physical Chemistry*; McGraw-Hill Companies Inc.: New York, 2002.
(5) Antonini, E.; Brunori, M. *Hemoglobin and myoglobin in their reaction with ligands*; North-Holland Publishing Co.: Amsterdam, The Netherlands, 1971.
(6) Asher, S. A.; Murtaugh, J. *J. Am. Chem. Soc.* **1983**, *105*, 7244.
(7) Keyes, M. H.; Falley, M.; Lumry, R *J. Am. Chem. Soc.* **1971**, *93*, 2035.
(8) Case, D. A.; Karplus, M. *J. Mol. Biol.* **1979**, *132*, 343.
(9) Schotte, F.; Lim, M. H.; Jackson, T. A.; Smirnov, A. V.; Soman, J.; Olson, J. S.; Phillips, G. N.; Wulff, M.; Anfinrud, P. A. *Science* **2003**, *300*, 1944.
(10) Dadusc, G.; Ogilvie, J. P.; Schulenberg, P.; Marvet, U.; Miller, R. J. D. *Proc. Natl. Acad. Sci. U.S.A.* **2001**, *98*, 6110.
(11) Peters, K. S.; Watson, T.; Logan, T. *J. Am. Chem. Soc.* **1992**, *114*, 4276.
(12) Peters, K. S. *Angew. Chem., Int. Ed.* **1994**, *33*, 294.
(13) Sakakura, M.; Yamaguchi, S.; Hirota, N.; Terazima, M. *J. Am. Chem. Soc.* **2001**, *123*, 4286.
(14) Terazima, M. *Pure Appl. Chem.* **2001**, *73*, 513.
(15) Ogilvie, J. P.; Plazanet, M.; Dadusc, G.; Miller, R. J. D. *J. Phys. Chem. B* **2002**, *106*, 10460.
(16) Miksovska, J.; Day, J. H.; Larsen, R. W. *J. Biol. Inorg. Chem.* **2003**, *8*, 621.
(17) Gibson, Q. H.; Ainsworth, S. *Nature* **1957**, *180*, 1416.
(18) Miller, R. J. D. *Acc. Chem. Res.* **1994**, *27*, 145.
(19) Armstrong, M. R.; Ogilvie, J. P.; Cowan, M. L.; Nagy, A. M.; Miller, R. J. D. *Proc. Natl. Acad. Sci. U.S.A.* **2003**, *100*, 4990.
(20) Anfinrud, P. A.; Han, C.; Hochstrasser, R. M. *Proc. Natl. Acad. Sci. U.S.A.* **1989**, *86*, 8387.
(21) Petrich, J. W.; Poyart, C.; Martin, J. L. *Biochemistry* **1988**, *27*, 4049.
(22) Henry, E. R.; Sommer, J. H.; Hofrichter, J.; Eaton, W. A. *J. Mol. Biol.* **1983**, *166*, 443.

(23) Gensch, T.; Viappiani, C. *Photochem. Photobiol. Sci.* **2003**, *2*, 699.
(24) Rovira, C.; Parrinello, M. *Int. J. Quantum Chem.* **2000**, *80*, 1172.
(25) Ogilvie, J. P.; Armstrong, M. R.; Plazanet, M.; Dadusc, G.; Miller, R. J. D. *J. Lumin.* **2001**, *94*, 489.
(26) Goodno, G. D.; Dadusc, G.; Miller, R. J. D. *J. Opt. Soc. Am. B* **1998**, *15*, 1791.
(27) Hagen, S. J.; Hofrichter, J.; Eaton, W. A. *Science* **1995**, *269*, 959.
(28) Hagen, S. J.; Hofrichter, J.; Eaton, W. A. *J. Phys. Chem.* **1996**, *100*, 12008.
(29) Librizzi, F.; Viappiani, C.; Abbruzzetti, S.; Cordone, L. *J. Chem. Phys.* **2002**, *116*, 1193.
(30) Sastry, G. M.; Agmon, N. *Biochemistry* **1997**, *36*, 7097.
(31) Dadusc, G.; Goodno, G. D.; Chiu, H. L.; Ogilvie, J.; Miller, R. J. D. *Isr. J. Chem.* **1998**, *38*, 191.
(32) Tian, W. D.; Sage, J. T.; Srajer, V.; Champion, P. M. *Phys. Rev. Lett.* **1992**, *68*, 408.
(33) Abbruzzetti, S.; Viappiani, C.; Bruno, S.; Mozzarelli, A. *Chem. Phys. Lett.* **2001**, *346*, 430.
(34) Ostermann, A.; Waschipky, R.; Parak, F. G.; Nienhaus, G. U. *Nature* **2000**, *404*, 205.
(35) Miller, R. J. D. *Annu. Rev. Phys. Chem.* **1991**, *42*, 581.
(36) Yoshisawa, M.; Suzuki, K.; Kubo, A.; Saikan, S. *Chem. Phys. Lett.* **1998**, *290*, 43.
(37) Nagasawa, Y.; Ando, Y.; Okada, T. *Chem. Phys. Lett.* **1999**, *312*, 161.
(38) Rosca, F.; Kumar, A. T. N.; Ionascu, D.; Sjodin, T.; Demidov, A. A.; Champion, P. M. *J. Chem. Phys.* **2001**, *114*, 10884.
(39) Wang, W.; Demidov, A.; Ye, X.; Christian, J. F.; Sjodin, T.; Champion, P. M. *J. Raman Spectrosc.* **2000**, *31*, 99.
(40) Zhu, L.; Li P.; Huang, M.; Sage, J. T.; Champion, P. M. *Phys. Rev. Lett.* **1994**, *72*, 301.
(41) Kachalova, G. S.; Popov, A. N.; Bartunik, H. D. *Science* **1999**, *284*, 473.
(42) Fraga, E.; Webb, M. A.; Loppnow, G. R. *J. Phys. Chem.* **1996**, *100*, 3278.
(43) Webb, M. A.; Kwong, C. M.; Loppnow, G. R. *J. Phys. Chem. B* **1997**, *101*, 5062.
(44) Markel, F.; Ferris, N. S.; Gould, I. R.; Myers, A. B. *J. Am. Chem. Soc.* **1992**, *114*, 6208.
(45) Agmon, N.; Hopfield, J. J. *J. Chem. Phys.* **1983**, *79*, 2042.
(46) Ansari, A.; Jones, C. M.; Henry, E. R.; Hofrichter, J.; Eaton, W. A. *Biochemistry* **1994**, *33*, 5128.
(47) Scott, E. E.; Gibson, Q. H. *Biochemistry* **1997**, *36*, 11909.
(48) Dansker, D.; Samuni, U.; Friedman, J. M.; Agmon, N. *Biochim. Biophys. Acta* **2005**, *1749*, 231.